# PROJECT FINAL REPORT

## Final publishable summary report

**Grant Agreement number:** 241384

**Project acronym:** HIPOCIGS

**Project title:** New concepts for high efficiency and low cost in-line manufactured flexible CIGS solar cells

**Funding Scheme:** FP7-ENERGY-2009-1

**Period covered:** from 01/01/2010 to 31/12/2012

**Dr. Friedrich Kessler, ZSW**

**Tel:** +49 711 7870 201

**Fax:** +49 711 7870 230

**E-mail:** friedrich.kessler@zsw-bw.de

**Project website address:** http://hipoCIGS.zsw-bw.de

*TABLE OF CONTENTS*

# 1 Executive summary

The present report presents results and highlights of the FP7 EU project hipoCIGS, insofar they are not confidential.

Except for module encapsulation all (main) deposition and process steps have been addressed which might be suitable for a future cost effective and highly efficient roll-to-roll processing of $Cu(In,Ga)Se_2$ (CIGS) based solar cells and modules. The CIGS absorber was deposited by the co-evaporation method only. Various CIGS coating plants were available from multistage small area batch to multistage medium area. Although on polyimide foil also roll-to-roll processing was possible, it was not a key focus of this project.

Since CIGS is grown at substrate temperatures between about 450°C and 650°C, desired and undesired diffusion of elements plays a major role during the absorber formation and thus the choice of substrate material strongly affects the film growths and process parameters. Most interesting substrate materials with regard to the fabrication of monolithically integrated modules were thin polyimide films (25 µm) for the low temperature processing at about 450°C and enamelled steel for the high temperature processing at 600 - 650°C. However, also aluminium and mild steel foils functioned, whereas enamelled aluminium has shown to be not well suited due to cost arguments and physical properties.

Best Na doping method at low substrate temperatures was the deposition of a thin NaF layer onto the finished CIGS layer followed by an annealing process. For the high temperature processing on enamelled steel the composition of the enamel layer itself was optimised in a way that it could serve as precursor layer.

An $In_2S_3$ buffer layer was evaporated from $In_2S_3$ powder on an area of up to 30cm x 30cm. On glass reference substrates a cell efficiency of up to 17.5 % was reached. Film growth is characterised by sulphur depletion, even if flash evaporation of the powder is applied.

An atmospheric pressure plasma-enhanced CVD method was successfully developed for the non-vacuum deposition of ZnO window layers. Results achieved so far are very promising and work will be continued.

Remarkable progress has been achieved in the low temperature co-evaporation of the absorber: So a small-area cell efficiency of 18.7 % was demonstrated both on polyimide and stainless steel foil, whereas 17.1 % and 15.4 % were reached on aluminium and mild steel foil, respectively. This means that – at least in the laboratory – the efficiency gap between low and high temperature CIGS processing could be closed. With an inline and high temperature CIGS processing on enamelled steel a maximum efficiency of 18.6 % could be achieved without additional external doping. To reduce material costs and deposition time the absorber thickness was reduced. Even with thin CIGS layers of only 0.9 µm and 1.24 µm on polyimide efficiencies above 15 % and 16 %, respectively, were obtained.

Monolithically integrated mini-modules with 8 – 52 interconnected cells have been fabricated on polyimide foil and enamelled steel substrates by using complete laser scribing on polymer and mixed laser/mechanical scribing on enamelled steel. On polyimide an efficiency of 14.8 % (8 cells in series) was achieved, on enamelled steel 15.4 % (16 cells) and 12.9 % (52 cells) was reached.

# 2 Summary of project context and objectives

***Project context***

At the stage of project application (2009) the photovoltaic (PV) market was maintaining an impressive annual growth rate of 30 – 50 % during the last few years. Continuously increasing production capacities, enhanced performance of solar modules and decreasing costs of solar modules were impressive testimonials of the technological success of conventional photovoltaic technology based on Si wafer technology. However, thin film PV technologies, comparatively less developed but having high potential for low production costs were drawing considerable attention. In 2008, the thin-film PV module production increased to 0.89 GW, a growth of 123% compared to the previous year.

All thin film solar cells can be grown on flexible foils (metal or polymer), provided they fulfil the minimum requirements for chemical, optical, structural and thermal characteristics. Flexible solar cells based on CdTe, CIGS, a-Si based, $TiO_2$-dye based, organic materials have been developed on different types of substrates. The highest CIGS solar cell efficiencies on foils are significantly higher than 6 - 13% achieved with other materials.

Flexible a-Si devices are available since more than fifteen years, however, at a module efficiency level of only 4 – 8 %. Thus, the CIGS technique was and still is the only thin-film technology which allows the fabrication of flexible devices with mean efficiencies clearly above 10 %. Flexible CIGS solar cells and modules could be made even more efficient and they offer a high potential for low manufacturing cost. The transfer of know-how and efficiencies from CIGS-on-glass to CIGS-on-foils, however, is challenging due to:

- high temperatures required for the formation of optimum absorbers (i.e. some foils cannot withstand the required high temperatures, or foils have intolerably large thermal expansion coefficient)

- contamination of the absorber by diffusion of undesired elements out of the flexible substrate in case of metal foils

- need of additional Na doping for the growing absorber (on glass substrates Na diffuses out of the soda lime glass into the CIGS)

- lack of a common, low-cost substrate with suitable mechanical, physical, and chemical characteristaics.

The highest efficiency of CIGS solar cells on various substrates are achieved by growing a sequence of layers such as a sputtered Mo back electrode, vacuum evaporated CIGS absorber, chemical bath deposited (CBD) CdS buffer layer and sputtered ZnO:Al/ZnO front contact. Different methods are used for incorporation of Na into CIGS to achieve the desired electronic properties for high photovoltaic conversion efficiency. High deposition temperatures of the CIGS layer normally are advantageous to achieve high semiconductor quality. On polyimide and metal foils, respectively, substrate temperatures of ~450°C and 550°C can be used for deposition of “high quality” CIGS layers. Enamelled steel substrates would allow the application of even higher temperatures up to 650°C. However, at such high process temperature thermal expansion mismatch of layers and substrates becomes a critical problem to achieve crack-free and defect-free structures. Optimum control of the composition in CIGS layers, microstructure (grain size), morphology and interface properties of adjacent layers including inter-diffusion and structural defects are the key issues for obtaining high efficiency solar cells.

Most of the R&D work on flexible solar cells including achievements of record efficiency solar cells, has been performed on small sized substrates and/or using static deposition methods (substrate remains at a fixed position). For industrial production, however, large area substrates (films or foils) are mandatory. They will be in motion during deposition of layers and

further processing with inline manufacturing processes. The transfer of laboratory-developed "static deposition" processes to "inline deposition" on moving substrates brings additional challenges as the "growth kinetics" and "chemical phase formation reactions" are drastically different and the control of the inhomogeneous evaporation /sputtering flux profiles becomes a very complex task.

Basically, **the challenge is to achieve high performance solar cells and low production costs** by overcoming the thermal mismatch and scaling-up problems, and to optimally control the structural, chemical, electrical and optical properties of multi-layers and interfaces.

The substrate plays an important role as it strongly affects all subsequent processes. Therefore a first important step was to modify, evaluate and optimise three different types of flexible and cost-effective classes of substrates such as polyimide films, mild steel or Al foils, and enamelled steel or Al foils with regard to thermal expansion, temperature stability, surface roughness, etc.

Polymer as well as metal foils have their specific advantages and disadvantages for use as substrates for flexible, monolithically connected solar modules. At the project start flexible solar cells with highest record efficiency of 14.1% on polymer films have been developed using a low temperature process, which has been shown also suitable for metal foils even without any impurity diffusion barrier layer. A goal of the project was to develop a low temperature CIGS process with a targeted solar cell efficiency of 16 %, which would be a new record and comparable to results on metal foils.

Another topic with view on cost reduction was to investigate the reduction of the CIGS thickness by a factor of two (≤ 1µm) without significant efficiency loss.

The overall conceptual roadmap started from already achieved research excellence in lab and lead to high efficiency low cost inline manufactured flexible solar cells and modules through innovative R&D and collaborative efforts by:

- Investigation of new flexible substrates for high performance and low cost flexible modules
- Evaluation of substrate texturing for optical confinements with the aim to reduce the absorber thickness
- Optimisation of CIGS and buffer properties and their interfaces by application of different characterisation methods
- Innovative high throughput growth processes for optimal control of the electro-optical characteristics through composition gradient in the absorber layer
- Improvement of more transparent alternative buffer layers, transparent conducting front contact layer and their interfaces for high performance cells
- Development and assessment of new interconnect technologies for processing of solar modules
- Assessment of the potential of the development and implementation in industrial production.

## Objectives

The main project goal was to develop novel layer deposition processes onto flexible substrates suited for inline and/or roll-to-roll production of highly efficient flexible solar modules using thinner (≤ 1 µm) CIGS absorber layer and with potential for low production costs below 0.6 €/Wp.

The research and development focused on new processes and layers for the advanced inline fabrication of highly efficient and cost-effective CIGS solar cells. All investigations and developments should be fully compatible with a roll-to-roll (R2R) production. However, the R2R deposition equipment itself was not an issue within this project. Also, the encapsulation/lamination technology was beyond the scope of these activities. At the end, the improvement of electronic materials properties and interfaces and the enhanced device and module efficiencies have to compete with cost arguments. That is, all new processes and enhanced understanding were used to reduce production costs with the aim of leveraging the flexible CIGS technology.

Important tasks were:

i) **Cost-effective substrates:** Development of high efficiency flexible solar cells and modules on low cost metal and polyimide substrates. Three novel types of cost effective metallic substrates were evaluated: mild steel (new), aluminium foil, and enamelled steel of different texture/morphology optimised for the CIGS requirements. Development of novel enamels suitable for high temperature processing in vacuum and selenium vapour. Selection of best polyimide film for suitable crack-free high efficiency cells, roll-to-roll processing at 450°C, and monolithic interconnection.

ii) **Implementing optical confinement effects:** Correlation of morphologies of substrates with layers and impacts on optical characteristics of layers and interfaces. Optimisation of the composition gradients in CIGS and interface properties with front- and back- electrical contacts.

iii) **Understanding of structural, chemical and electronic properties**: The optimisation of high quality low- and high-temperature deposited CIGS on novel textured metal foils and polyimide films. Different methods of sodium doping and a deep understanding of this process, the role of impurities from substrates, their diffusion behaviour and interfaces. Design of an optimised CIGS deposition process and implementation of Na incorporation for achieving ~16% efficiency cells on polyimide (target for a new world record efficiency on polymer substrate)

iv) **Improved device efficiencies with very thin CIGS absorbers**: Development of growth processes and solar cell structures of different thicknesses and their impact on solar cell performance.

v) **Reduced materials consumption:** Reduction of the CIGS absorber thickness by a factor of about 2 without reduction of the photocurrent.

vi) **New and roll-to-roll-compatible processes:** Inline evaporated $In_2S_3$-based buffer in combination with i-ZnO or ZnMgO. Fast processing, scale-up, transfer to roll-to-roll processing.

vii) **Reduced processing time,** e.g. by thinner layers (e.g. CIGS), high-speed deposition methods (e.g. TCO) and by preventing vacuum breakage for buffer layer.

viii) **Novel TCO's:** Atmospheric Pressure Plasma Enhanced CVD reactor and process for natively textured ZnO:Al optimised for low temperature and high deposition speed. Metal grid embedded TCO front contacts for interconnect.

ix) **Interconnect technology for solar modules:** Monolithic series interconnection by laser scribing. Cell interconnection via advanced "wafer technique". Hybrid approach combining scribing and metal grids. Fast processing, scale-up, transfer to roll-to-roll processing.

# 3 Main S&T results/foregrounds

## 3.1 Alternative substrates, back contact and Na supply

***Advanced substrate materials and Na supply***

Sodium (Na) plays a crucial role in CIGS solar cells increasing cell efficiency mainly driven by enhancing the open circuit voltage $V_{oc}$ and the fill factor FF of the cells. On standard rigid glass substrates sodium diffuses out of the glass substrate through the Mo back contact into the CIGS layer during layer growth at high substrate temperatures. As this diffusion process is thermally activated cell efficiency is lower on glass substrates in a low temperature CIGS process. On Na free substrates like polyimide, steel or Aluminium foil, Na has to be supplied externally. Different methods of sodium supply have been tested to evaluate the best way of Na supply on large area for industrial applications:

- Na supply by evaporation of NaF during or after the CIGS process
- Na supply by sodium doped Molybdenum (Mo:Na)
- Na supply by enamel layer

***External Na supply by NaF in a low temperature CIGS process***

To investigate the influence of NaF on CIGS solar cells, Na free polyimide foil was used as substrate and coated with CIGS in a multi-stage low temperature CIGS process at EMPA [1]. NaF was supplied during the first, second or third stage of a multi-stage CIGS process (labeled during 1st, 2nd, or 3rd stage in the following) and electronic properties of the resulting solar cells were investigated. In addition a further device was fabricated with Na added after the CIGS process by NaF post deposition treatment (PDT). The PV parameters on each sample of this series are given in Tab. 1. It has to be noted that the used multi-stage co-evaporation process was originally optimized to achieve highest efficiency when Na is added during a PDT. Therefore, better performance of the device with Na PDT could be expected, because Na influences the interdiffusion kinetics of the elements which results in an altered In/Ga composition grading profile as well as different defect formation.

*Tab. 1: PV parameters of best performing solar cells on polyimide foil (with antireflective coating) obtained with different Na incorporation methods. Average $V_{oc}$ and FF are given in brackets.*

| **Na addition** | **1st** | **2nd** | **3rd** | **PDT** | **Record PDT** |
|---|---|---|---|---|---|
| $J_{SC}$ (mA cm$^{-2}$) | 24.8 | 24.7 | 26.6 | 32.1 | 34.8 |
| $V_{OC}$ (mV) | 628 (633) | 631 (630) | 661 (659) | 697 (692) | 712 |
| FF (%) | 73.7 (73.8) | 74.8 (74.2) | 73.7 (73.9) | 76.5 (76.0) | 75.7 |
| Efficiency (%) | 11.5 | 11.7 | 13.0 | 17.1 | 18.7 |

[1] A. Chirilă et al., Nature Materials 10 (2011) 857, DOI: 10.1038/NMAT3122

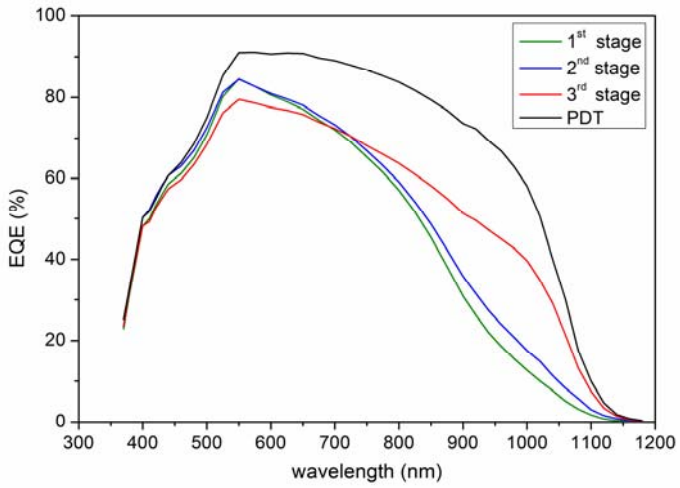


*Fig. 1: External quantum efficiency curves of CIGS solar cells with Na added in different stages of the absorber deposition process.*

When Na was added during the CIGS growth process, performance of the solar cells was lower. The device with Na added during the 3rd stage performed better compared to the devices with Na added during 1st and 2nd stage. Best PV performance was achieved when Na was supplied after the CIGS process during a PDT. In this series all devices with Na added during the CIGS growth showed low $J_{sc}$ (expected ~30-32 mA/cm$^2$). External quantum efficiency (EQE) measurements were performed to investigate the origin of the low $J_{sc}$. As shown in Fig. 1 the devices with Na added during CIGS growth exhibit weak collection of photons in the wavelength range from 550 to 1100 nm. Such a behavior could origin from large defect concentration in the absorber together with a small space charge region, which results in increased recombination of generated electron-hole pairs. An altered In/Ga grading profile compared to the "optimized" profile in the sample with NaF PDT could reinforce this effect. A record efficiency of 18.7 % could be achieved on polyimide foil with Na supply by PDT as well as on stainless steel.

### *External Na supply by Mo:Na in a low temperature CIGS process*

Sodium doped Mo layers (Mo:Na) were tested in a low temperature CIGS process as Na source. The efficiency could be enhanced from 9.2 % for the Na free solar cell to 13.8 % (without anti-reflective coating) for a solar cell with a Mo:Na layer. Hence Na supply by Mo:Na layers also works in a low temperature CIGS process [2].

### *External Na supply by an enamel layer in a high temperature CIGS process*

Enamelled steel substrates were developed and optimized as advanced substrates for CIGS solar cells and modules. The multifunctional enamel layer acts as corrosion protection, as insulating layer to enable monolithic integration on the conducting steel substrate, as diffusion barrier and as alkali source for the CIGS layer. Enamelled steel substrates (the enamel layer contains Na and K) were tested as Na source in a high temperature inline multistage CIGS process at ZSW and compared to standard glass substrates (Na and low K content) and mild steel substrates (alkali free). The PV parameters of the resulting cells are shown in Tab. 2.

[2] R. Wuerz et al., Thin Solid Films 519 (2011) 7268, DOI:10.1016/j.tsf.2011.01.399

Without any diffusion barrier, the conversion efficiency on mild steel is zero, as all cells were shunted. In contrast, the cells on enamelled steel show even higher efficiencies than cells on the glass reference substrate [3]. On enamelled steel the open-circuit Voltage $V_{oc}$ and the short-circuit current density $J_{sc}$ are higher compared to the glass reference substrate (see Tab. 2).

*Tab. 2: PV parameters of CIGS cells with $MgF_2$ antireflective coating on steel substrates with and without enamel layers and on glass reference substrate. Fe concentration [Fe], Na concentration [Na] and signal intensity of K39 in the CIGS layer as measured by SIMS.*

| substrate | $Na_2O$ | $K_2O$ | $\eta_{max}$/ % | $V_{oc}$/ mV | *FF*/ % | $J_{sc}$/ mA $cm^{-2}$ | [Fe]/ ppm | [Na]/ ppm | K39/ cps |
|---|---|---|---|---|---|---|---|---|---|
| mild steel | no | no | 0.0 | 1 | 0.0 | 2.0 | 839 | 1.7 | 253 |
| enamel | yes | yes | 16.8 | 730 | 71.6 | 32.0 | 3 | 130 | 34808 |
| glass | yes | low | 15.0 | 654 | 74.6 | 30.7 | 1.5 | 140 | 1702 |

SIMS measurements revealed that Na and K diffused out of the enamel layer into the CIGS layer (see Tab. 2) and that the enamel layer blocks the diffusion of Fe, as intended. Capacitance versus voltage measurements revealed a higher net charge carrier density in the CIGS layer on enamelled steel compared to the glass reference [3] which is caused by the higher K content in the CIGS layer on enamel (both samples have a similar Na content). Therefore one has to take into account not only the Na content but the whole alkali content in the CIGS layer for the interpretation of the results.

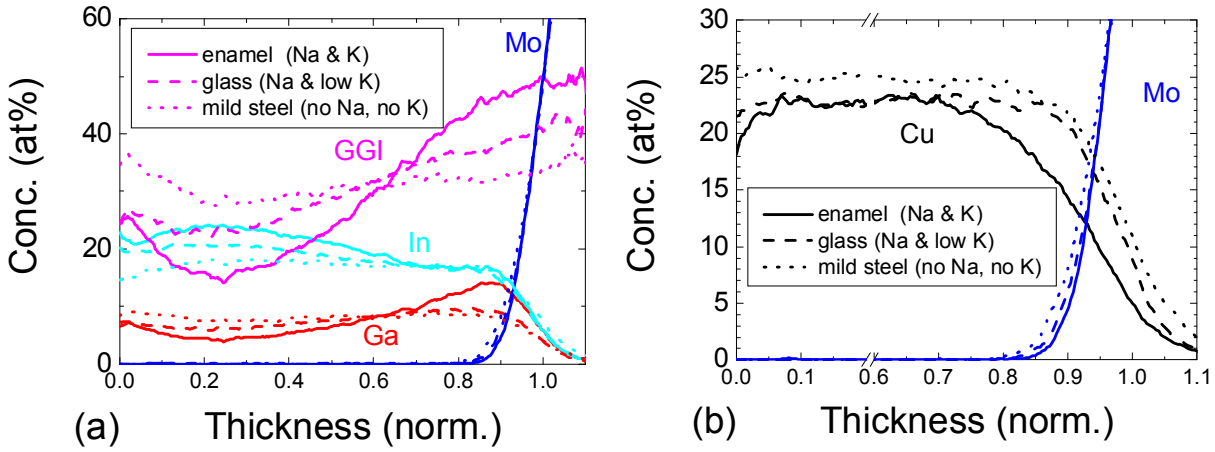


*Fig. 2: Concentration profiles of a) In (cyan), Ga (red), GGI (magenta) and Mo(blue) and b) Cu (black) for CIGS layers on enamelled steel (solid curves), glass reference substrate (dashed curves) and mild steel reference substrate (dotted curves). The thickness (x axis) has been normalized for better comparison of the profiles. The CIGS layer on the enamelled steel with the highest alkali content shows the highest In content and strongest GGI gradient. (Note the break in the x-axis of Fig. 2b).*

In Fig. 2 the concentration profiles (derived from SNMS measurements) on the three different substrates are shown together with depth profiles of the relative [Ga]/([Ga]+[In]) concentrations abbreviated by GGI. The GGI gradient decreases with decreasing alkali content

[3] R. Wuerz et al., Solar Energy Materials and Solar Cells 100 (2012) 132, DOI:10.1016/j.solmat.2012.01.004

in the CIGS layer. Hence not only Na but also K hinders interdiffusion of Ga and In during the multistage growth of the CIGS layer. The higher In content in the CIGS layer on enamelled steel compared to the layer on the reference substrates (also found by XRF, not shown here) leads its having a lower band gap, and hence a higher $J_{sc}$. The integral copper content (measured by XRF) of the CIGS layer on the steel reference (24.3 %) is much higher compared to the layer on glass (22.3 %) and enamel (21.2 %) (see Fig. 2b), hence the Cu content decreases and the In content increases with increasing alkali concentration. The high copper content in the layer on the steel reference (even 25.4 % was measured with SNMS in the surface region, see Fig. 2b) might be the reason for the shunted cells of this sample (see Tab. 2), as $Cu_{2-x}Se$ precipitations could shunt the cells. At the Mo/CIGS interface the Cu signal of the CIGS layer on enamel (solid black curve in Fig. 2b) decreases already at lower depth towards the CIGS/Mo interface compared to the layer on glass (dashed black curve) and mild steel (dotted black curve). Here the Cu has not completely diffused to the back of the CIGS layer as on the layer on glass and mild steel. From this we conclude that even the diffusion of Cu into the $(In,Ga)_2Se_3$ layer formed during the first stage of the layer growth is hindered due to the presence of K, as the Na content in the CIGS layer on enamel and glass is similar (see Tab. 2). With help of enamel layers a cell efficiency of 18.6 % could be reached (see below).

The supply of Na and K for CIGS layers by enamel layers only works in a high temperature CIGS process. If the substrate temperature of the CIGS process is too high or heating and cooling ramps are too fast, shrivelling of the enamel layers occurs and hinders cell and module production.

***Impact of sodium on doping level of the absorber***

Results of capacitance profiling show a correlation between the amount of supplied sodium and apparent hole concentration in the absorber. In the presence of Na hole concentration increases from around $10^{14}$ $cm^{-3}$ (Na-free device) to around $10^{16}$ $cm^{-3}$ (Fig. 3). All methods of Na supply are adequate to achieve this level of hole concentration. A model explaining how non-passivated grain boundaries can affect apparent doping level has been proposed and verified by simulations shown in Fig. 4.

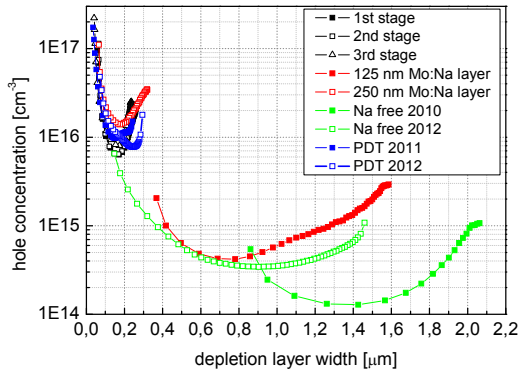


*Fig. 3: Hole concentration profiles of the cells with various Na supply methods, calculated from capacitance measurements. The results include Na free cells, cells with Mo:Na precursor layers and cells with Na supplied during or after the absorber growth.*

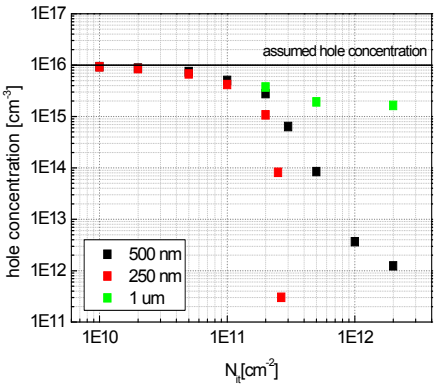


*Fig. 4: Simulated hole concentration in the $Cu(In,Ga)Se_2$ absorber with 250 nm, 500 nm and 1 µm grains and the same, equal to $10^{16}$ $cm^{-2}$ shallow acceptor concentration. Donor states (5 x $10^{11}$ $cm^{-2}$ at $E_v$+0.88 eV) at the grain boundaries have been assumed.*

***Conclusions***

- NaF post deposition treatment is the best method for Na supply of CIGS layers with NaF in a low temperature CIGS process
- Na supply with Mo:Na even works in a low temperature CIGS process.
- Enamelled steel works well as an alkali source in a high temperature CIGS process only
- K hinders diffusion of metal elements during growth of CIGS layers
- higher apparent doping level in the absorbers with sodium might be explained by passivation of the grain boundaries.

## 3.2 High quality CIGS at low and high substrate temperature

Maximising throughput for roll-to-roll manufacturing of highly efficient CIGS solar cells and modules on flexible substrates is highly important for the industry and it potentially leads to low cost solar electricity generation in the near future. While currently the growth of 2 µm-thick CIGS layers for high efficiency devices takes typically 30-60 min in research labs, the industrial production requires significantly shorter deposition time (< 10 min) for high-throughput manufacturing. The necessary drastic increase in deposition rate is expected to influence the physical properties of CIGS layers and performance of the solar cells.

Fig. 5 shows the cross section of a CIGS solar cell. The p-type semiconductor CIGS layer is sandwiched between a metallic electrical contact at the back side and n-type semiconductor as well as a transparent electrical contact at the front side. The tasks for obtaining high quality CIGS solar cells are to investigate experimentally the growth kinetics, inter-diffusion phenomena and physical properties of CIGS layers, chemical and microstructural properties of hetero-junctions and opto-electronic characteristics of solar cells grown at very high deposition rates. Moreover, reduction of the absorber thickness from 2 µm to below 1 µm without significant performance losses (< 10 % in relative efficiency) should significantly cut material losses per production unit and indirectly decrease the deposition time. CIGS layers were grown at different substrate temperatures using in-line suitable evaporation processes. The principle of the deposition equipment for the elemental co-evaporation process is sketched in Fig. 5 on the right side.

The relevance of this task was not only to gain fundamental scientific insights into the materials, interfaces and devices but also to develop highly efficient flexible solar cells on different cost effective substrates and to facilitate high throughput roll-to-roll manufacturing in the future for benefits of both industry and customers. CIGS depositions at low substrate temperature (between 370°C to 450°C) and high temperature (above 550°C) are optimised for "high structural, electronic and optical quality" CIGS layers to yield record efficiency solar cells in research labs and process knowledge for industrial implementation at a later stage.

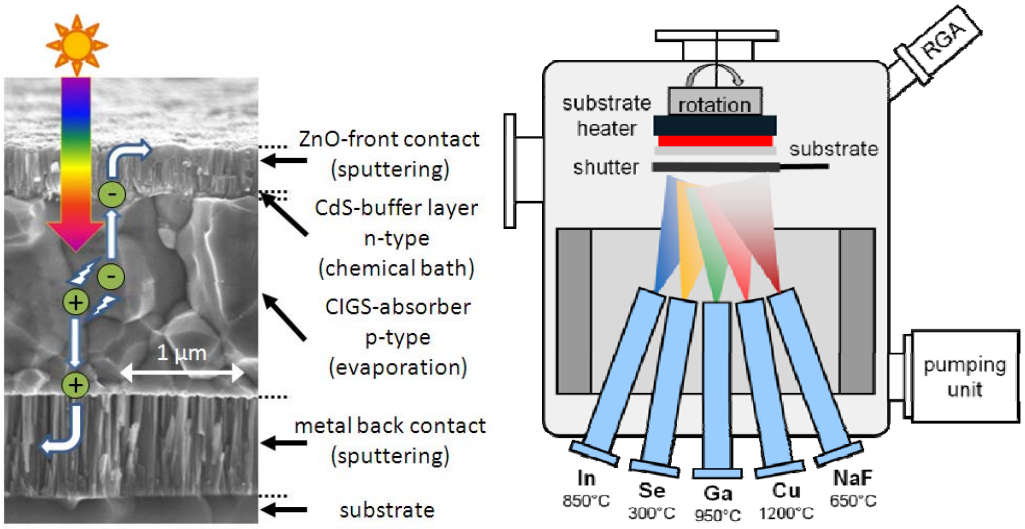


*Fig. 5: Schematic cross-section of a CIGS solar cell showing all involved layers and deposition methods (left). Schematic of the deposition equipment used to grow CIGS layers and incorporation of sodium (right).*

### 3.2.1 Low temperature CIGS on polyimide, steel, Al, and enamelled Al foils

Suitable roll-to-roll suitable substrates, such as polyimide and aluminium foils, require low deposition temperatures (~400°C), which restricts significantly the achievable high efficiency, especially for very high deposition rates. This is because both the growth behaviour and layer properties are known to change drastically at low substrate temperatures. The structural and electronic properties of CIGS layers deposited at low temperature are therefore not of "sufficiently high quality" to yield high efficiency solar cells.

#### *CIGS solar cells on polyimide film*

Extensive process development has been carried out for the growth of high quality absorber layers at low substrate temperature. An efficiency of 17.6 % on polyimide has been achieved over the course of 2010 [4,5,6] and has been further improved to 18.7 % [1] within the scope of the hipoCIGS project (Fig. 6).

[4] A. Chirilă et al., 35th IEEE PVSC, Honolulu, 2010, pp. 657-660.
[5] A. Chirilă et al., 25th EUPVSEC / 5th WCPEC, Valencia, Spain, 3BV.2.68, 2010.
[6] A. Chirilă et al., Prog. Photovolt. Res. Appl. 19 (2011) 560, DOI: 10.1002/pip.1077.

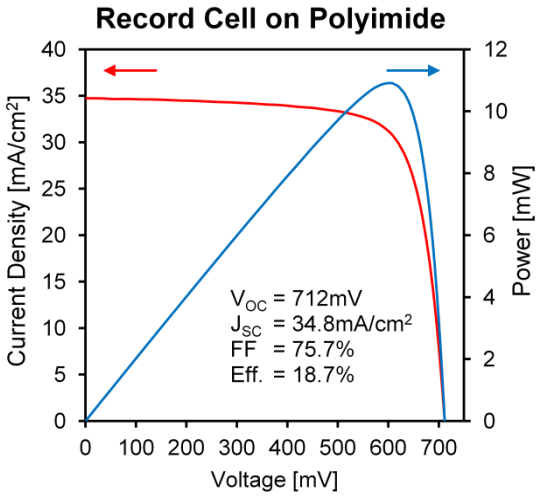


*Fig. 6: J-V and P-V measurements of the 18.7 % efficiency record device on polyimide film together with the characteristic PV parameters. The measurement has been certified by the Fraunhofer Institute ISE, Freiburg, Germany.*

### *CIGS solar cells on steel foil*

The low temperature multistage process has also proven to be suitable for stainless steel substrates where an independently measured efficiency of 18.7 % has been achieved without additional diffusion barrier between the Mo back contact and the stainless steel substrate.

On mild steel it was possible to obtain 15.4 % efficiency with the low temperature multistage evaporation process when using an additional diffusion barrier.

### *CIGS solar cells on bare Al foil*

Commercially available Al foil (99.9 % purity) was used as substrate and coated with a diffusion barrier layer prior to the Mo back contact deposition. CIGS was grown with a similar multi-stage process as developed for polyimide films. The low substrate temperature is expected to further hinder detrimental Al diffusion into the absorber layer. Initial experiments resulted in a 14.1 % efficiency device on Al-foil. On that sample, no apparent cracks or delamination was observed.

With a diffusion barrier layer configuration it was possible to achieve an efficiency of up to 17.1 % (Fig. 7).

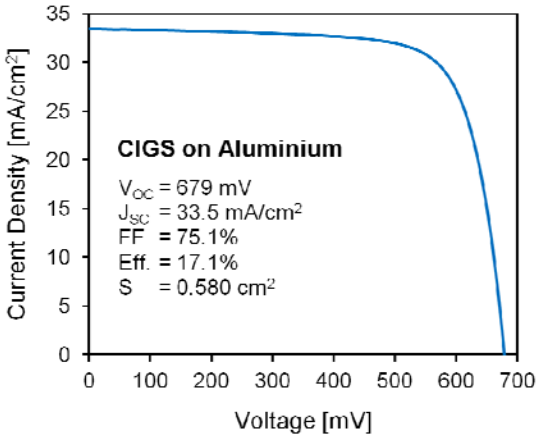


*Fig. 7: J-V characteristics of the best solar cell obtained on Al foil (with $MgF_2$ antireflective coating).*

### *CIGS solar cells on enamelled Al substrates*

Enamelled Al sheets from PEMCO were coated with a Mo back contact and then with a CIGS layer in a low temperature CIGS process. Nevertheless the enamel layer cracked during the CIGS process, the CIGS layer peeled off and cell processing was not possible. Hence this task was stopped.

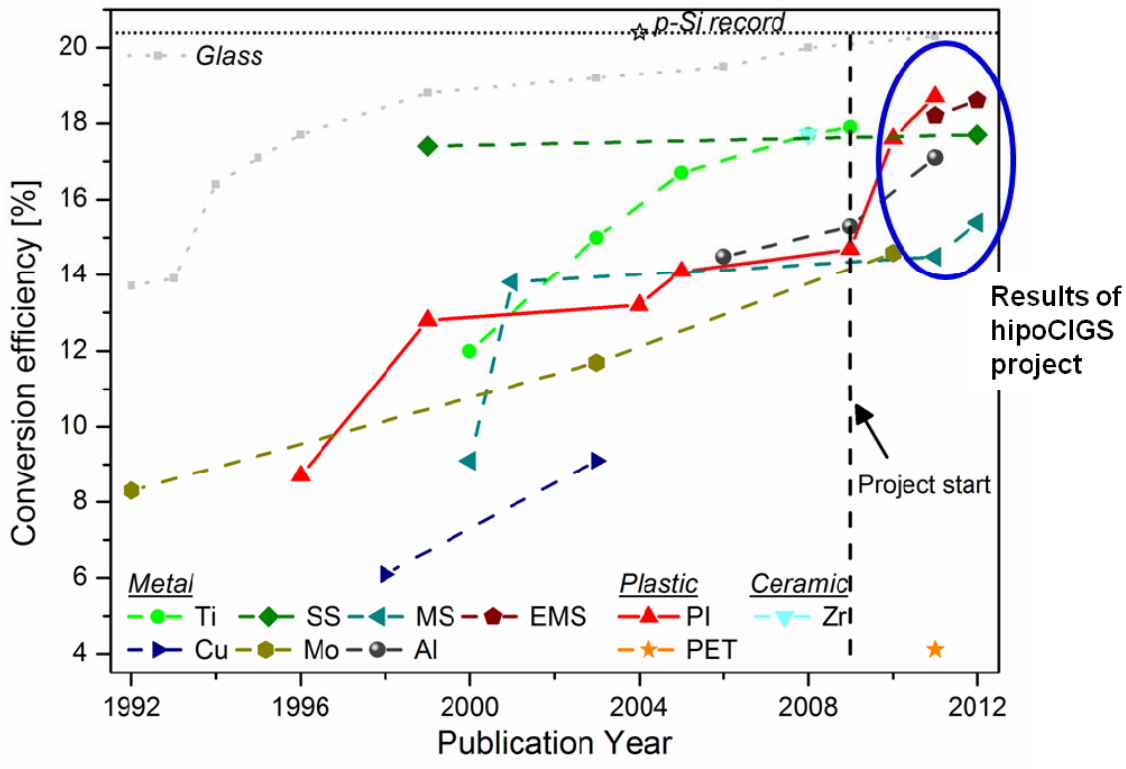


*Fig. 8: Evolution of the conversion efficiencies of CIGS thin film solar cells on various types of flexible substrates. Also shown are the record values for CIGS solar cells on rigid glass substrate and the reference value of polycrystalline silicon solar cells.*

Fig. 8 summarizes the published record efficiencies of flexible CIGS solar cells on different substrate materials. The dashed black line in Fig. 8 indicates the start and the blue ellipse shows the achievements of the hipoCIGS project. The project partners were able to demonstrate substantial improvement of CIGS solar cells on all investigated substrate materials in the hipoCIGS project and developed new record efficiencies.

Key to the abovementioned achievement was to tailor the compositional gradient along the CIGS film depth, in particular the [Ga]/([Ga]+[In]) ratio. Adapting this ratio changes the electronic band gap structure and the developed process enables to fabricate similar band gap profiles which in prior art have only been achieved using high temperature growth processes.

The modification of the [Ga]/([Ga]+[In]) profile [1] has been found to be the key in order to remove an electronic barrier in the device structure and to reduce recombination losses which have constrained device performance to significantly lower values.

### *CIGS solar cells with reduced absorber layer thickness*

The record devices mentioned above are achieved with typically about 3 µm thick CIGS layers. During the first half of the hipoCIGS project, the process has been scaled down proportionally in time by a factor of 2 and compared to baseline reference samples. Fig. 9 shows the J-V curves of the best devices obtained. Even though an efficiency decrease of about 10 % relative is observed, a 15.5 % efficiency device with 1.4 µm thick CIGS has been achieved. The work on absorber layer thickness reduction was closely tied to WUT in order to understand limiting factors of such thin absorber layers.

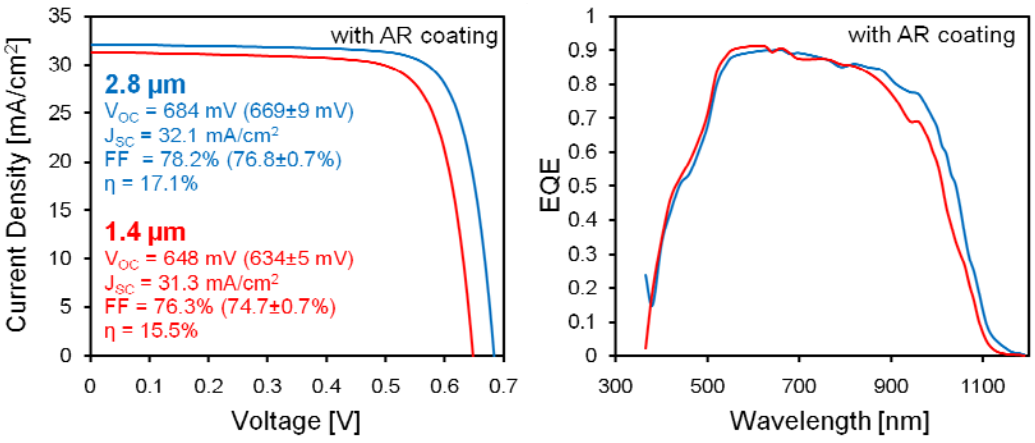


*Fig. 9: J-V and EQE measurements of solar cells on polyimide comparing a baseline device (2.8 µm) with an absorber of reduced thickness (1.4 µm), mean values are given in brackets.*

In the second half of the hipoCIGS project, a simpler modification of the multistage process was used for the deposition of CIGS layers with a thickness slightly below 1 µm on polyimide substrates. In this modified process the rates of the 1st and 3rd stage were not equal, but constant over the whole respective stage and the amount of Cu-excess [7] has been varied from 25 % to 75 %, and the whole process was aiming at a final Cu-content of 0.8 ([Cu]/([Ga]+[In]) ratio). The 3rd stage duration was longer for samples with higher Cu-excess, and the 1st stage shortened accordingly in order to obtain a similar final thickness for all samples. J-V curves of

[7] S. Seyrling, A. Chirila, D. Güttler, F. Pianezzi, P. Rossbach, A.N. Tiwari, Modification of the three-stage evaporation process for $CuIn_{1-x}Ga_xSe_2$ absorber deposition, Thin Solid Films, 519, 7232-7236, 2011.

the obtained cells with different Cu excess are presented in Fig. 10, and compared with a sample with standard thickness prepared under similar conditions. Anti-reflection coating was used for all samples presented in this study.

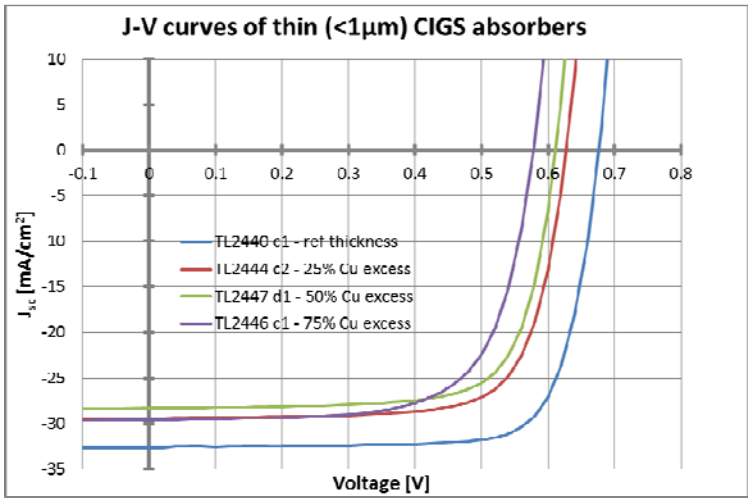


*Fig. 10: J-V curves of the best cells with thin absorber obtained with maximal Cu-excess amounts of 25 %, 50 % and 75 %, and of a thick reference sample prepared under similar conditions with efficiency of 17 %.*

In all samples with thin CIGS layers (about 0.8 µm) some absorption losses are expected to occur. This is reflected in the short circuit current value, where the slightly thinner 50 % Cu excess sample also shows a slightly lower $J_{sc}$ compared with the two other samples. The best sample with reduced CIGS layer thickness shows a 20 % loss compared to the reference run. This study shows that lower maximal Cu-excess is beneficial for the device performance. This is also in agreement with what has been observed for standard absorber thickness.

Based on the results discussed above, further experiments have been conducted with further reduced Cu-excess in the 2nd stage. With this, efficiencies above 15 % have been achieved with absorbers as thin as 0.9 µm. Compared to the reference device, only $J_{sc}$ losses are observed. Furthermore, efficiencies above 16 % have also been achieved with absorbers with 1.24 µm thickness.

### *High deposition rates for the CIGS absorber layer*

Further work concerning high deposition rates have been carried out in the hipoCIGS project. To gain preliminary insights into the critical growth phases, an investigation has been carried out on glass substrates at a low temperature suitable for polyimide foils. A basic three stage process has been used and the deposition rates during either the 2nd stage or the 3rd stage have been increased drastically to about 500-600 nm/min CIGS growth rate [8]. In both cases the relative efficiency loss as compared to a baseline process was found to be in the range of only about 10 % as shown in Fig. 11.

[8] A. Chirilă et al., Prog. Photovolt. Res. Appl. 20 (2012) 209, DOI: 10.1002/pip.1122.

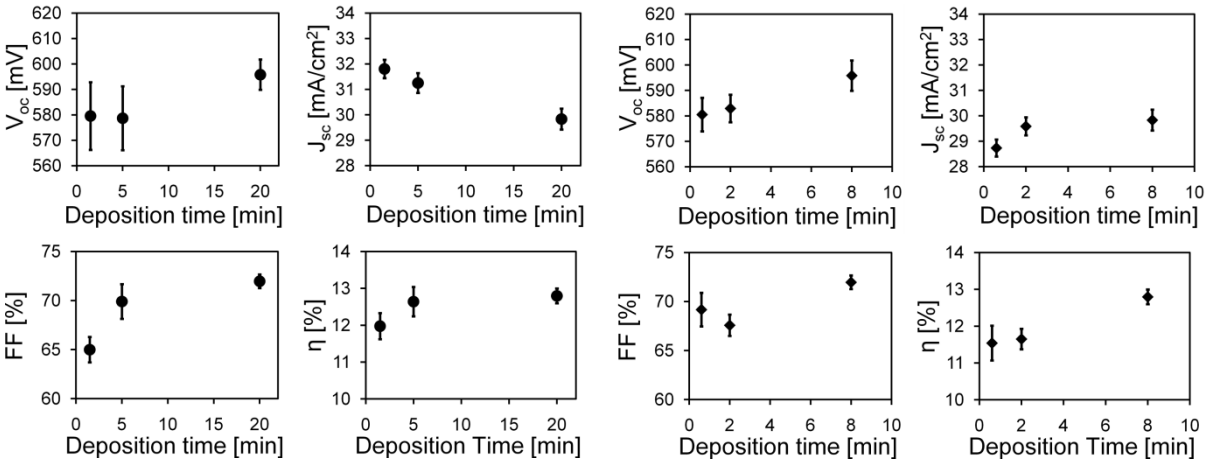


*Fig. 11: J-V parameters of solar cells with different deposition times during the 2nd stage (left) and during the 3rd stage (right) of a three stage process.*

Standard deposition time for absorbers with thickness of 1 µm is 20 min. An objective of the project is to achieve higher evaporation rates in order to reduce standard deposition time (30-60') for a thicker absorber below 10', with less than 20 % efficiency loss. Evaporation rates (up to 4x) have been used separately for each stage, keeping the rates in the other respective stages as usual. The goal was to look at the influence of higher rates in each stage on final device properties, as described above and published in [8]. It was found that higher rates (up to 10x) in 1st and 2nd stage do not deteriorate the device significantly, but that on the other hand the 3rd stage was more critical.

If the deposition time for each fastest stage is added, a total deposition time of 6' is shown to be feasible. Higher deposition rates are not excluded either and further work should be done to understand these aspects even better. A deposition time below 10 min was shown to be feasible with less than 20 % efficiency loss compared to our record efficiency device.

***CIGS absorber layers deposited by high speed roll-to-roll process***

At ZSW a roll-to-roll setup was implemented which started working in April 2010. In this setup, CIGS thin-film solar cells on polyimide foil have been processed without vacuum break between the deposition of the Mo and the CIGS layer. Na doping was realized by using sodium-doped Molybdenum (Mo:Na). The deposition time for the CIGS layer was 30 minutes with a resulting thickness of about 2.3 µm. Solar cell processing was finished outside of the roll-to-roll pilot-line by chemical bath deposition of CdS for the buffer layer and by sputtering of ZnO for the front contact layer. During the ZnO:Al sputtering a metallic mask was used to define the cell area of about 0.5 cm². An Al grid was applied by electron beam evaporation through a shadow mask.

Efficiency increased from 2.7 % in the beginning up to 10.3 % in April 2011.

After ramp-up of the system, the main task was to enhance reproducibility and to increase efficiency by optimization of the CIGS process and Na supply as well as to enhance the adhesion. The improved process yielded a cell efficiency of 12.6 % without antireflective coating (ARC) (see Tab. 3). With ARC coating the cell efficiency amounts to 13.1 %.

*Tab. 3: Solar cell parameters of the best CIGS cells on polyimide foil with CIGS from roll-to-roll pilot-line at ZSW (with Al grid): maximum efficiency $\eta_{max}$, short-circuit current density $J_{sc}$, open-circuit voltage $V_{oc}$, fill factor FF; $MgF_2$ was used as antireflective coating (ARC).*

| Sample ID | $MgF_2$ ARC | $\eta_{max}$/ % | $V_{oc}$/ mV | *FF*/ % | $J_{sc}$/ mA $cm^{-2}$ | cell area/ $cm^2$ |
|---|---|---|---|---|---|---|
| 120614_9 | no | 12.6 | 540 | 73.3 | 31.9 | 0.5 |
| 120614_9 | yes | 13.1 | 536 | 72.6 | 33.7 | 0.5 |

Flisom's manufacturing facility uses substrate rolls of polyimide. The polyimide web is unrolled within a vacuum co-evaporation system where it is brought up to the temperature required for the multiple stage material deposition sequence. During the deposition sequence the polyimide web passes over a series of heated evaporation sources. Since the web is constantly in motion, the spacing of the sources, the plume of evaporated material they produce, and the heat they contribute is crucial to a successful CIGS layer production.

A first objective to increase throughput was to achieve consistent, homogeneous, and uniform deposition over a wide web. The distribution of material as it exits the nozzle of a source is usually non uniform. Ways to improve distribution uniformity include nozzle shaping, non-uniform heating of the evaporation source, and possibly using masks to prevent contamination by excess material dispersed away from the web.

Two-dimensional CIGS layer composition and important compositional ratio parameters such as [Cu]/([Ga]+[In]) and [Ga]/([Ga]+[In]) were mainly investigated using X-ray fluorescence measurements (XRF). This has enabled us to tune the design and positioning of its sources paving the way to increased photovoltaic conversion efficiencies thanks to improved layer composition. After the first half of the hipoCIGS project Flisom was able to manufacture uniform CIGS layers over wide polyimide substrates.

Another challenge lies in the ability to handle wide webs. During its course from one roll to the other within the vacuum deposition system, the polyimide substrate undergoes changes in temperature that induce substantial web expansion in the hot zone. Flisom took special care to *design and adjust web handling processes*, mechanisms, and temperature control to cope with changes in the web's mechanical properties. Changes to the vacuum deposition system have enabled us to prevent the occurrence of artefacts detrimental to the deposited layer's quality.

The main focus of the second period was then on two objectives: a) reduction of CIGS deposition time by higher growth rates and b) reduction of CIGS absorber thickness without significant performance loss. From an industrial viewpoint those two goals are important since they have a direct influence on increasing CIGS deposition throughput and on material consumption, and therefore have the potential to reduce production cost. All steps were done roll-to-roll in stand-alone machines, which means that the foils were rolled and unrolled at each deposition step. A schematic of the process steps is shown in Fig. 12.

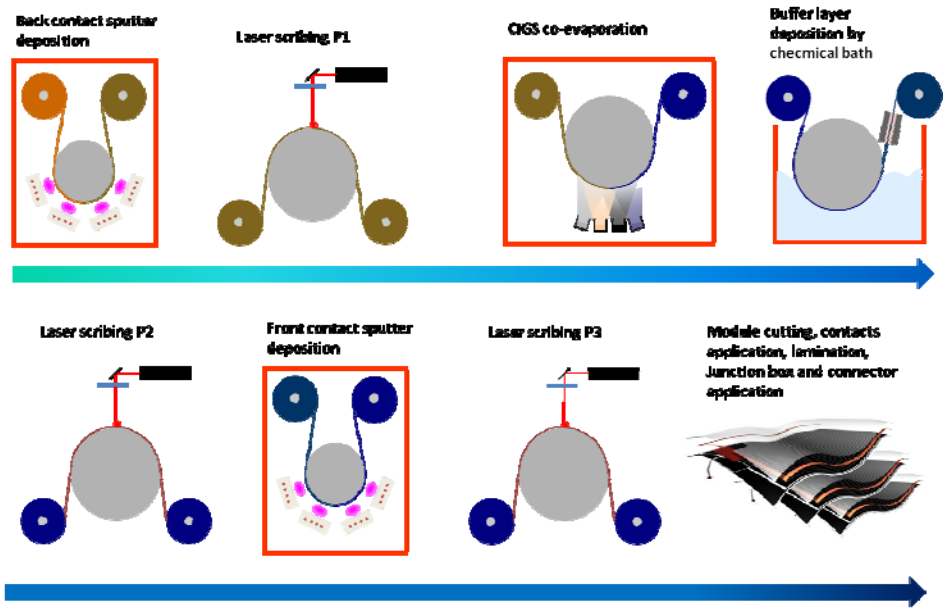


*Fig. 12*: *Schematic of manufacturing steps at Flisom.*

### 3.2.2 High temperature CIGS on steel and enamelled steel foils

***CIGS solar cells on enamelled steel substrates***

Enamelled low carbon steel substrates from PEMCO were coated with CIGS in an inline multi-stage pilot line at ZSW in a high temperature CIGS process (T ~ 600°C). In the first half of the hipoCIGS project the highest cell efficiency on enamelled steel substrate reached was 17.6 % (confirmed by ISE, see Fig. 13a).

The efficiency on the enamelled substrates was in most cases even higher than on the glass reference substrate. In the second half of the project with an optimized grid (3 % shadowing) and a further development of CIGS solar cells on enamelled steel substrates, the maximum efficiency on enamelled steel substrate could be further enhanced to 18.6 % (Fig. 13b), which is again even higher than the value on the glass reference substrate (18.3 %). This reveals the high potential of enamelled steel as an alternative to glass substrate for CIGS thin-film solar cells.

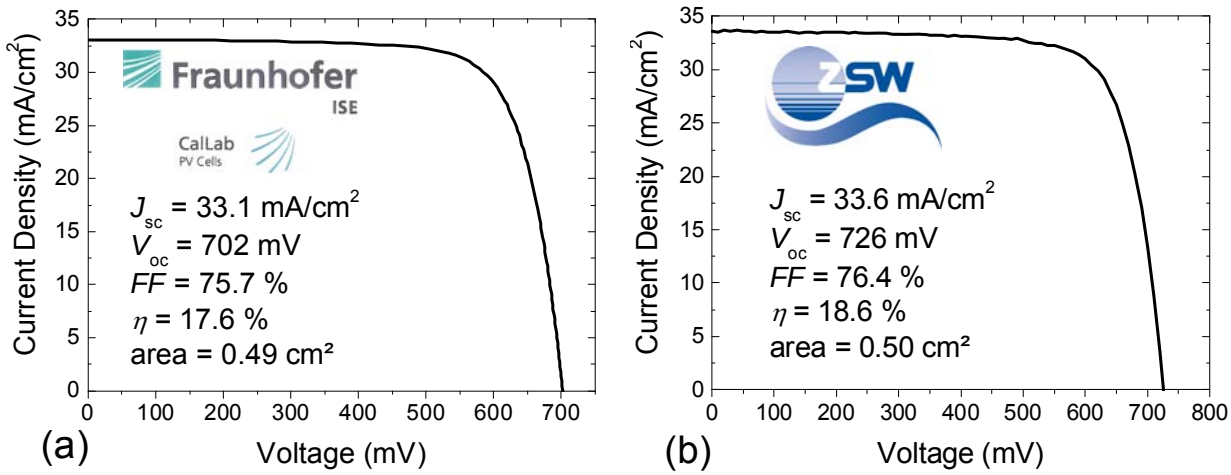


*Fig. 13: JV-curve of record cells on enamelled steel substrate a)sample 6308-1 (from first project period) as confirmed by ISE and b) sample 6308-15 (from second project period) as measured at ZSW.*

### *CIGS solar cells with reduced absorber layer thickness*

In a first step ZSW produced CIGS solar cells on glass with a standard thickness of 2.5 µm and then with a low thickness of 0.7 µm by enhancing the substrate carrier velocity in the inline pilot line. The cell efficiency decreased from 17.4 % to 12.1 % for a thickness reduction from 2.51 µm to 0.74 µm, respectively (Fig. 14a). Hence a reduction of CIGS thickness by 70 % leads to only 30 % loss in efficiency. The main loss was observed in the short circuit current density $J_{sc}$. The quantum efficiency measurements (Fig. 14b) reveal that the main losses of charge carrier collection occur in the infrared region. Hence, recombination in the bulk and at the back contact has to be reduced.

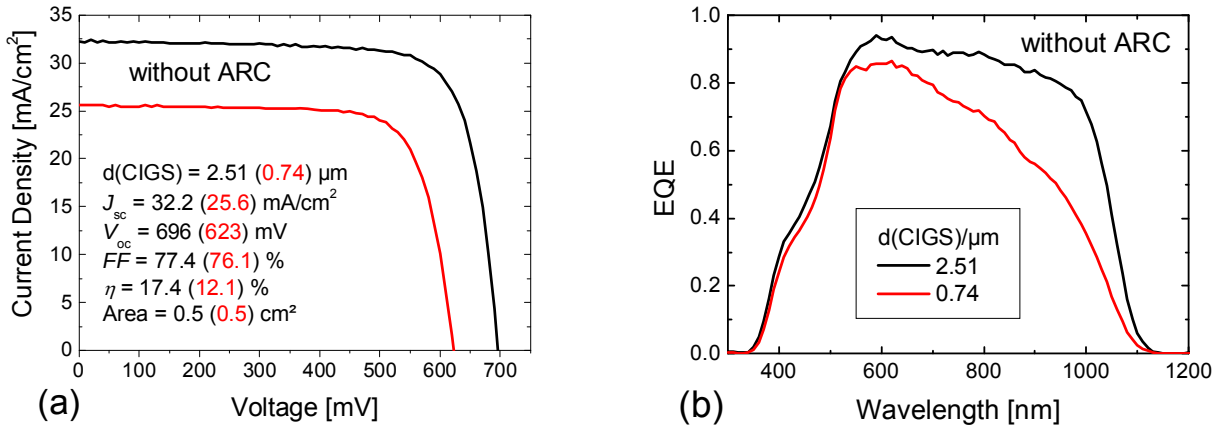


*Fig. 14: Effect of CIGS thickness reduction on a) J-V curve and cell parameters and on b) external quantum efficiency for CIGS solar cells from inline multi-stage pilot line at ZSW on glass substrate.*

### 3.2.3 Conclusion

In the scope of the hipoCIGS project remarkable progress was achieved in the field of flexible CIGS solar cells. The collaborative project allowed knowledge-driven improvement of the laboratory as well as the pilot production deposition processes based on new insights obtained by correlation of electrical device analysis and material characterization. The CIGS deposition process at low substrate temperatures at EMPA suitable for polyimide, steel and Al foils has been improved, yielding:

- Certified efficiency of 18.7 % achieved on polyimide film,
- Independently measured efficiency of 18.7 % achieved on stainless steel foil,
- In-house measured efficiency of 17.1 % achieved on aluminum foil,
- In-house measured efficiency of 15.4 % achieved on mild steel foil

With roll-to-roll deposition equipment at ZSW a solar cell efficiency of 13.1 % on polyimide substrates was obtained.

The partners could identify the critical deposition stages which also include the method of Na doping (see chapter 3.1). It was possible to prove also for the low temperature CIGS process the deposition time can be significantly reduced. For high rate deposition, EMPA demonstrated the role of each stage in the multistage deposition process on the device performance.

By further modifying the low temperature multistage deposition process, CIGS solar cells with absorber layer thickness below 1 µm were obtained with 15.4 % efficiency. Compared to the reference device (17.0 %), this means an efficiency loss of less than 10 %. The results from the collaborative effort indicate that flexible solar cells with CIGS deposition time below 10 min and layer thickness below 1 µm yielding an efficiency of more than 16 % are feasible.

In a high temperature inline multi-stage CIGS process at ZSW an in-house measured efficiency of 18.6 % was achieved on enamelled steel.

In most cases efficiency on enamelled steel was even higher compared to the efficiency on soda lime glass substrate showing the high potential of enamelled steel as an alternative substrate for CIGS solar cells and modules.

## 3.3 Evaporated indium sulphide buffer layers

Chemical bath deposition (CBD) is state-of-the-art for the deposition of the CdS buffer layer in CIGS solar cells. An alternative vacuum-routed process is searched for to make the production step compatible for in-line deposition manufacturing. In the project, physical vapour deposition (PVD) processes were investigated. At the same time CdS was replaced by $In_2S_3$, an alternative buffer material with higher absorption in the short wavelength region.

In the project, the alternative buffer layers were deposited by two different evaporation techniques:

- Continuous thermal evaporation (ZSW) and
- In-line flash evaporation (EMPA)

The resulting $In_xS_y$/CIGS/Mo/glass substrates were completed with a sputtered iZnO/ZnO:Al window and an Al-grid layer. The solar devices were analyzed for their IV-characteristics under AM1.5 condition. Thereby the influence of heat treatment by post-annealing steps was

investigated. Furthermore composition measurements by EDX and RBS were applied to the buffer layers to reveal composition changes of the indium sulphide source powder during evaporation and their influence on the cell characteristics.

Warsaw University of Technology (WUT) performed advanced electrical characterization including current-voltage analysis in the 120-330 K temperature range and capacitance methods like capacitance profiling and admittance spectroscopy, respectively, to gain information on dominating transport mechanisms and voltage distribution in the devices. The aim was to determine which particular properties were most severely limiting the performance of $In_2S_3$-buffered cells.

For continuous evaporation compound $In_2S_3$ powder was deposited by thermal evaporation in an in-line system. The main part of experiments was performed on glass substrates with laboratory cell devices to evaluate optimum process conditions for the buffer deposition. To demonstrate the scalability of the process to module area, mini-modules up to 30 x 30 cm² substrates were processed. The suitability of the buffer material and the deposition process was also demonstrated by roll-to-roll manufacturing CIGS cells on polyimide.

Process reproducibility is an important factor for manufacturing. In Fig. 15 the efficiencies of laboratory cells are shown which were processed in consecutive buffer deposition runs from one crucible filled with $In_2S_3$ powder. During the deposition series no obvious change of the cell efficiency is observed. It has to be mentioned that after the 39 deposition runs there was still some powder left in the crucible. In other experiments it was observed that the cell performance can drop when the powder starts to vanish and the layers get too thin. To prevent the degradation in an in-line manufacturing system a suitable re-filling procedure has to be used. Nevertheless, the result is very promising in regard of reproducibility of the continuous evaporation process.

Fig. 15 shows efficiency values of post-annealed cells. A post-annealing step in air at ~200°C is necessary to enhance the cell performance. Fig. 16 shows the IV performance of an example cell before and after the annealing.

Advanced electrical characterization of the samples before and after post deposition annealing showed that annealing reduced recombination via interface states but in most cases interface recombination was still contributing to the performance losses. It was facilitated by significantly higher effect of tunnelling to interface states in comparison to CdS reference cells indicated by higher ideality factors and weakly temperature-dependent saturation current. Properties of the buffer-window electrical characteristics were not affected by the annealing and no secondary barriers limiting carrier flow in case of thin enough buffer were detected. We concluded that a process of reconstruction of the interface takes place during annealing, which reduces the number of interface states. The importance of diffusion and exchange of elements between buffer and absorber remains to be investigated by other than electrical methods. Achieving similar efficiency on both CdS reference and $In_2S_3$-buffered cell when buffer deposition was carried out immediately after CIGS deposition with only shortly breaking the vacuum shows how foreign species (oxygen?) accumulated at the interface can disturb this process of interface reconstruction.

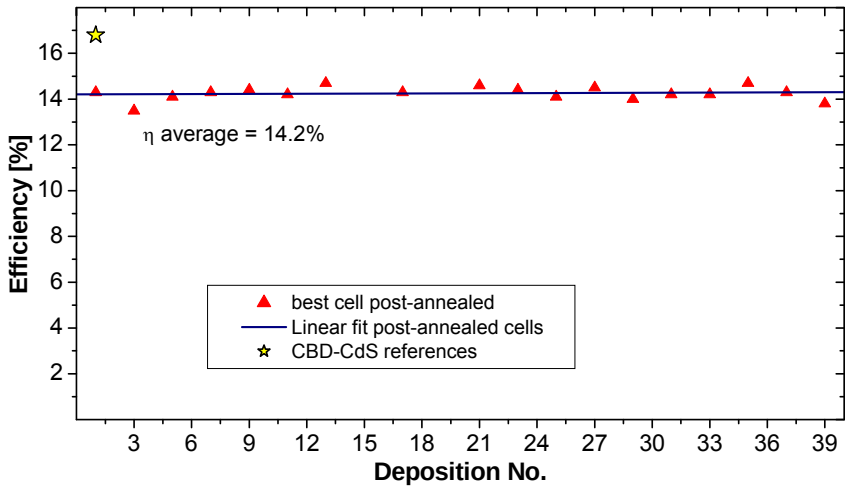


*Fig. 15. Efficiencies and fit of post-annealed cells with $In_2S_3$ buffer layer, deposited in a series from one crucible filling with $In_2S_3$ powder (CdS reference value is shown in comparison).*

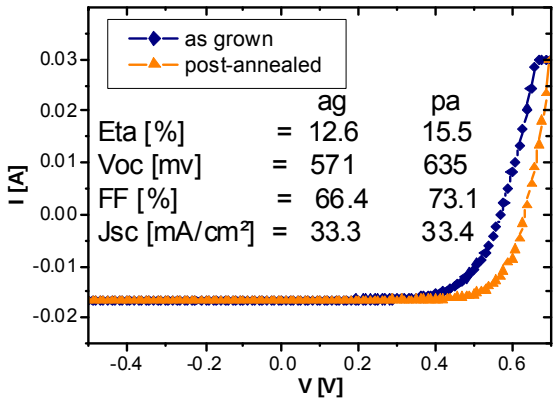


*Fig. 16. IV curves and characteristics of a cell with $In_2S_3$ buffer layer before and after annealing.*

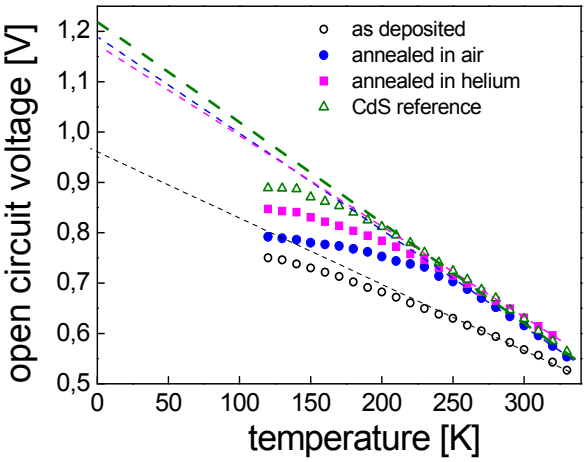


*Fig. 17. Effect of post-deposition annealing in air and in helium on open circuit voltage of PVD $In_2S_3$-buffered devices in comparison to the CdS-buffered reference cell.*

Compared to the CdS reference marked in Fig. 15 the devices with $In_2S_3$ buffer show a lower efficiency. This is mainly due to a lower open circuit voltage. During the project various process variations for the buffer and the adjacent absorber and window layer were performed to optimize the cell performance. The time between the process steps also plays a role.

For example, the buffer thickness has a significant influence on the cell performance. All IV parameters decrease with increasing thickness. Impact of buffer thickness on transport and photovoltaic parameters was interpreted as resulting from unfavourable voltage drop over the buffer occurring for too thick (>20 nm) buffers. The fill factor losses depended severely on the spectral content of illumination and were enhanced in case of “red” light (absorbed only in CIGS). These findings were interpreted as a result of both highly doped layer of absorber at

interface (p+ layer) together with lightly doped buffer on voltage distribution in the device and were supported by simulations with SCAPS software (Fig. 18).

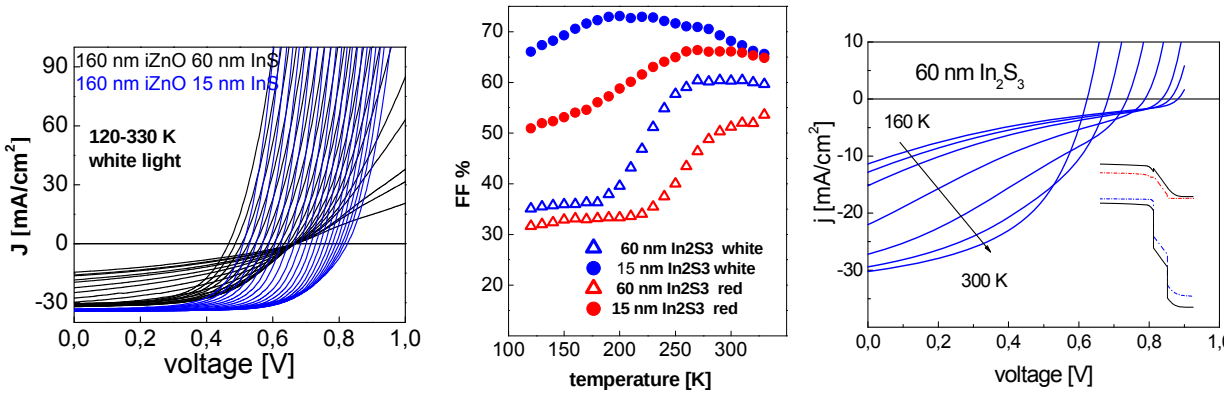


*Fig. 18. Comparison of the current-voltage characteristics under white light for devices with thick and thin PVD $In_2S_3$ buffers (left); fill factors as a function of temperature for devices with thick and thin PVD buffers under red and white light (middle); current-voltage characteristics together with band diagram of a cell with thick buffer simulated within p+ layer model (right).*

Another important issue is the composition of the $In_xS_y$ buffer layer. According to the different vapour pressures of the two elements indium and sulphur the initially stoichiometric powder compound $In_2S_3$ - in pellet form - will lose its sulphur content rather quickly. So, the ratio [S]/[In], which in the used powder form is 1.5, will constantly drop.

Transmittance and reflectance measurements, in combination with composition analysis by RBS and EDX on flash evaporated buffers revealed a phase transition of the $In_xS_y$ with decreasing sulphur content. Investigations of the effect on the cell performance for the different phases showed higher efficiencies for phases with lower sulphur concentration.

Fig. 19 shows the IV curve and data of the best cell device obtained during the project with a PVD $In_xS_y$ buffer layer by continuous evaporation and an optimized window. A new record efficiency of 17.5 % with AR-coating was achieved. The device showed a comparable performance to the CdS reference.

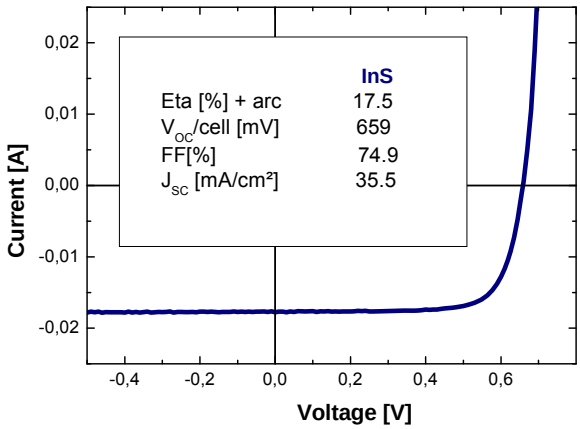


*Fig. 19. IV curve and data of the best cell device with $In_xS_y$ buffer layer on glass substrate (with ARC).*

The $In_xS_y$ buffer deposition process was applied to flexible substrates. Next to cell devices on polyimide web a monolithically interconnected mini-module with eight cells and flash evaporated $In_xS_y$ buffer was processed. The project partner Flisom developed a laser scribing equipment which allows accurate positioning of the scribe lines on flexible substrate material.

For performance comparison a standard device with CdS buffer layer was produced. For the CIGS device with CdS buffer layer, the extensive efforts in process optimization of CIGS growth and Na incorporation method yielded a mini-module efficiency of 13.3 % on 13 $cm^2$ area (Fig. 20). The performance of the mini-module with $In_xS_y$ buffer layer (13 $cm^2$ area) is also presented in Fig. 20. After white light soaking the mini-module with $In_xS_y$ buffer layer reaches a remarkable conversion efficiency of 10.6 %.

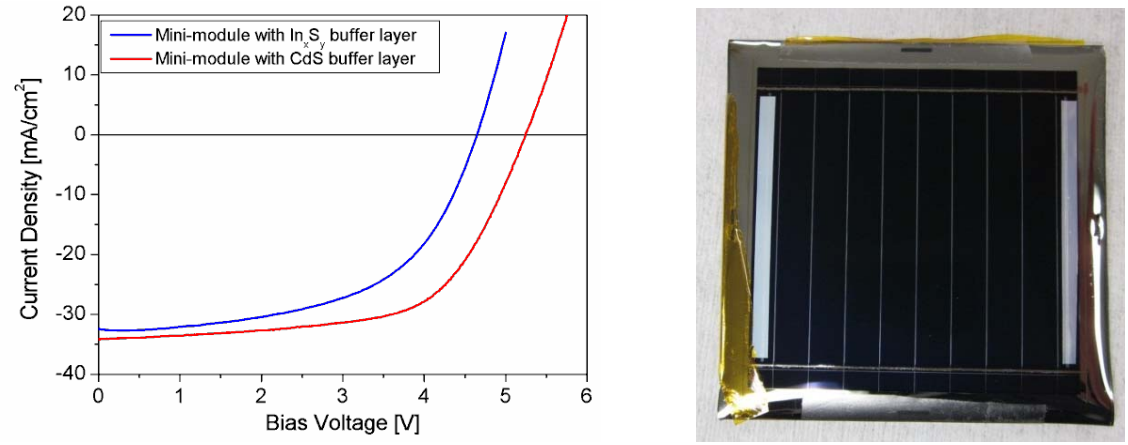


*Fig. 20. left: JV characteristics of CIGS mini-modules with CBD-CdS (red) and flash evaporated $In_xS_y$ (blue) buffer layers. Right: Photograph of the monolithically integrated mini-module with $In_xS_y$ buffer layer.*

In summary promising results were achieved for CIGS devices with PVD $In_2S_3$ buffer layers. Although for most experiment series the performance of the Cd-free devices was lower than the references, it demonstrated that high efficiency devices can be processed comparably to cells

with CdS. To achieve an optimized cell performance it is very important to adapt the properties of the combined absorber-buffer-window layer system.

### 3.4 Series interconnection of cells on polyimide, steel, and enamels

In order to obtain practically useful voltages, single solar cells have to be connected in series to form higher voltage solar modules. This part of the project presents different approaches of series interconnection of cells and the achieved results on the development of solar modules.

Deposition of a metal grid on large CIGS cells cut from a roll-to-roll coated substrate enables an approach to manufacture solar modules that is similar to that used with crystalline silicon cells. Following deposition of a metal grid, large solar cells can be series-connected using busbars, thereby resulting in a solar module. This method requires less tuning than so-called monolithic interconnects and offers the advantage that solar cells can be sorted according to their photovoltaic characteristics. This manufacturing process, however, does not take full advantage of the continuity of roll-to-roll production and requires rather sophisticated handling. Thin-film solar cells such as CIGS offer the option of monolithically integrated series interconnects between cells. Thin-film layers that compose the cell are patterned into stripes at successive production stages. The series interconnection is achieved by the sequence of deposition and patterning steps. This method can only be used on non-conducting substrates because the cells must be electrically separated at the back contact layer.

Three different laser scribing steps are necessary for **monolithic interconnection** of individual solar cells into solar modules. The scribed materials as shown in Fig. 21 are: back contact (metal); CIGS absorber (semiconductor); front contact ZnO:Al (TCO). At each laser scribing step, care must be taken not to damage the underlying thin layer or foil. Due to the fact that a large number of individual solar cells have to be series-connected, electrical contact resistance of the interconnections between the front contact of a first cell and the back contact of an adjacent second cell should remain low to limit total resistance loss. Good results were achieved with all-laser monolithic integration showing good reproducibility of the laser scribing process and a large process window to ensure reliable laser ablation even if material properties change. The scribes have to be aligned as near to each other as possible to minimize the "*dead area*".

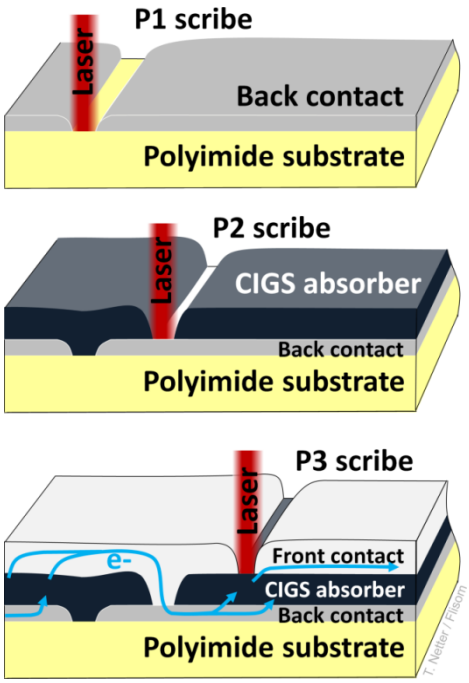


*Fig. 21: Monolithical interconnection by laser scribing.*

Usually, no conductive grid is required due to the small width of the single cells, typically about 5 mm. However, a **hybrid approach** was explored in this project, where a grid is deposited onto the front contact of monolithically-interconnected cells. The high conductivity of the grid allows larger cell widths, reducing both the patterning effort (thus increasing patterning throughput substantially) and the electrically inactive area used for the interconnect. In addition the TCO front contact can be made less conductive and therefore more transparent. Another reason to use a hybrid approach is that it enables larger cells resulting in higher current and lower voltage at same power output. Voltage or current can therefore be tuned by increasing the area of single cells and by reducing the number of series-connected cells.

The grids required for the single cell and the hybrid approach are typically deposited by screen printing. Due to temperature limitations on the curing process set by the CIGS device, the conductivity of these screen-printed grids is limited, and relatively thick gridlines are required as a result. **Electrochemical deposition of grid lines** directly onto the front contact was explored in this project as a way to achieve grids with a much better conductivity, allowing narrow grid lines, thereby allowing more light to reach the absorber and thus higher efficiency. However, although divided in smaller cells with measured efficiencies up to 12 %, electro-deposited grids showed shunting on larger cells and still lower efficiencies than for cells without a grid. Although SEM analyses did not yield evidence for CIGS degradation, further development and optimisation is therefore needed.

Mini-modules resulting from the collaboration between EMPA, which took care of layer deposition, and Flisom, which completed the laser scribing steps, were developed with a record efficiency of 14.8 % (aperture area). The solar modules were grown on polyimide substrates and comprised 8 monolithically interconnected cells. IV-curve and PV parameters are shown in Fig. 22.

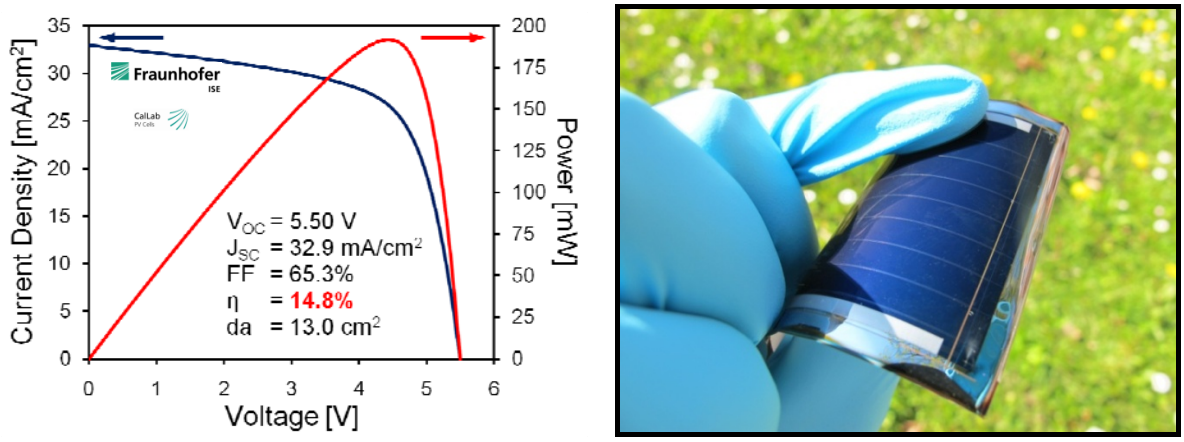


*Fig. 22: IV-curve and PV parameters (left) of a 4 x 4 cm² mini-module (right) with a record conversion efficiency of 14.8 %, which was independently certified by Fraunhofer ISE.*

At ZSW, CIGS modules on enamelled steel substrates have been developed using the enamel as alkali source and a high temperature multi-stage inline CIGS process. P1 scribing was realised with a ns-laser, P2 and P3 by mechanical scribing with a stylus. A best module efficiency of 15.4 % could be achieved on a 10 x 10 cm² enamelled steel substrate (Tab. 4). An efficiency of 12.9 % was achieved on a larger 23 x 30 cm² enamelled steel substrate (Fig. 23).

*Tab. 4: IV parameters of monolithically interconnected CIGS modules on enamelled steel substrates and glass reference substrates.*

| Substrate | active area / cm² | $\eta$/ % | $V_{oc}$/cell/ mV | $FF$/ % | $J_{sc}$/ mA cm$^{-2}$ | $V_{oc}$/ V | No of cells |
|---|---|---|---|---|---|---|---|
| glass | 6.4x7.4 = 47.0 | 13.9 | 697 | 68.4 | 29.2 | 6.97 | 10 |
| enamel | 7.5x8.2 = 61.3 | 13.9 | 695 | 68.3 | 29.2 | 11.1 | 16 |
| enamel with ARC | 7.5x8.2 = 61.3 | **15.4** | 714 | 71.5 | 30.1 | 11.4 | 16 |
| glass | 26.8x27.4 = 734.0 | 11.6 | 677 | 63.5 | 26.9 | 38.6 | 57 |
| enamel | 20.5x24.9 = 510.6 | **12.9** | 698 | 66.8 | 28.1 | 36.3 | 52 |

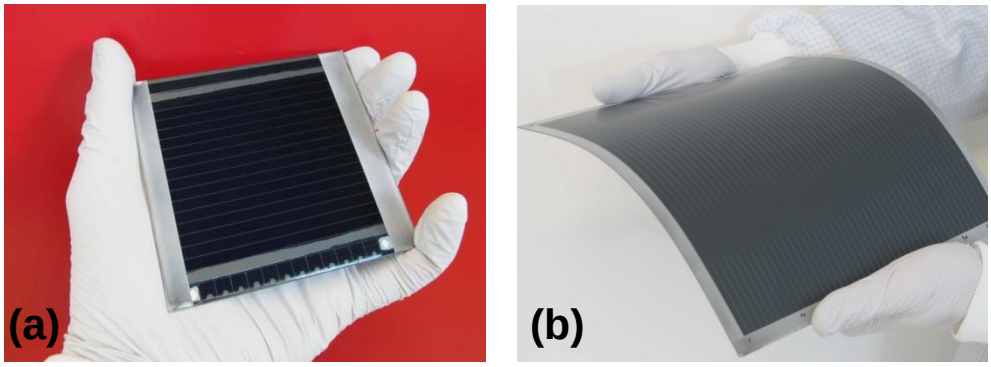


*Fig. 23: Modules on enamelled steel with a substrate size of a) 10 x 10 cm² and b) 23 x 30 cm².*

*Fig. 24: Solar modules of various sizes and designs developed by Flisom.*

Within the hipoCIGS project, Flisom has developed by complete roll-to-roll manufacturing a range of flexible modules of monolithically-interconnected cells for typical applications such as mobile electronics, mobile power, and building-integrated photovoltaics (Fig. 24).

To conclude, monolithic interconnection has demonstrated excellent results in terms of conversion efficiency, reliability, and reproducibility on polyimide as well as on enamelled steel substrates. This will make it possible to maximise the active area of solar modules and therefore to reduce module efficiency losses when compared to modules resulting from assemblies of single cells. The laser scribing process is fast, can be automated, and can be integrated into a roll-to-roll manufacturing process, thereby avoiding sorting or additional complex handling steps at the end. We therefore see monolithical interconnection as the method of choice for cell interconnection on insulating substrates. In certain cases a hybrid approach (monolithical interconnection of cells with metal grids) may be beneficial in terms of production cost or for special applications.

## 3.5 Atmospheric pressure PECVD ZnO as conductive window layer

CIGS cells basically exist of a CIGS absorber layer sandwiched between two electrodes. The back electrode facing the substrate may be opaque and is typically a Mo metal film. The front electrode facing the sun needs to be both transparent and electrically conductive.

Regarding the front electrode of CIGS cells, (industry) state-of-the-art is to apply transparent conductive oxide (TCO) films, mostly aluminum doped ZnO, by means of PVD processes in vacuum.

Low cost atmospheric pressure (AP) CVD processes have been developed for ZnO:Al, but at temperatures, above typically 400°C, which are too high to be compatible with thermally sensitive materials, such as CIGS solar cells and polymer substrates for flexible solar cells in general. Low temperature plasma enhanced (PE) CVD deposition of aluminum or boron doped ZnO has been developed, however under low pressure conditions.

TNO developed a low temperature CVD process for deposition of un-doped ZnO films, which become sufficiently conductive for application as front electrode after a UV treatment.

The films were deposited with an AP PE CVD injector in a lab-scale Watkin Johnson moving belt reactor, at a belt speed in the range of 20 to 60 mm/min and a substrate temperature of 200°C. Precursor was diethylzinc ($Zn(C_2H_5)_2$, DEZ) and the oxidant de-ionized $H_2O$. The deposition rate was 7 nm/s.
The as-deposited ZnO films were not conductive but became so during a short exposure (a few minutes) to near-UV radiation. The resulting films have a transparency of 90 % (Fig. 25) and a resistivity of 1.5 $10^{-3}$ Ohm cm, which over a large range is not film thickness dependent. A 1200 nm thick film had a sheet resistance of 15 ohm square.

These properties are measured shortly after the UV post treatment and decrease when the films are exposed to air. The latter can be prevented however by application of a thin (in the range of 50 to 100 nm thick) $Al_2O_3$ barrier layer.

Stacks of photo-induced conductive ZnO and $Al_2O_3$ barrier films have been tested as front electrode on CIGS test cells from ZSW on glass substrate. The $Al_2O_3$ barrier layer was applied by means of a spatial-ALD (atomic layer deposition) process. The performance of these cells was similar to those of CIGS cells from the same batch with a sputtered ZnO:Al film (Fig. 26 and Tab. 5).

*Tab. 5: I-V characteristics measured by ZSW for cells with reference sputtered ZnO:Al layer and UV-treated AP PE CVD applied ZnO TCO & $Al_2O_3$ barrier layers stack.*

| | η (%) | Voc (mV) | FF (%) | jsc (mA/cm²) |
|---|---|---|---|---|
| UV treated ZnO | 15,4 | 678 | 74 | 30 |
| reference | 15,5 | 696 | 71 | 31 |

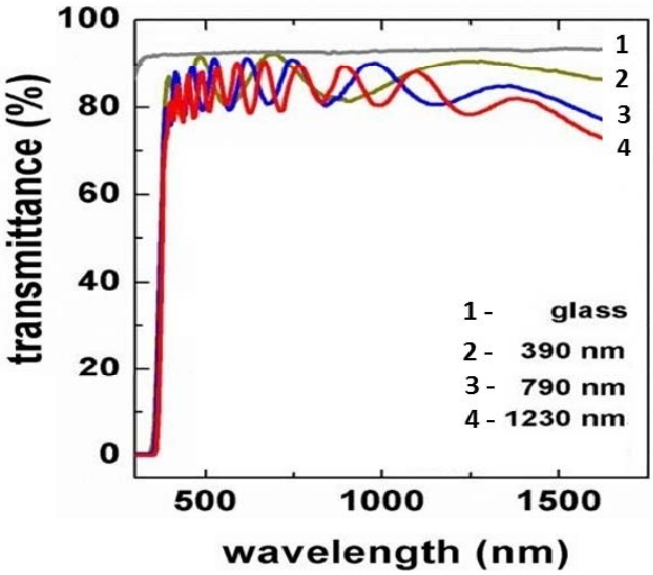


*Fig. 25: Transmittance of ZnO films on (0.7 mm thick boron-silicate) glass.*

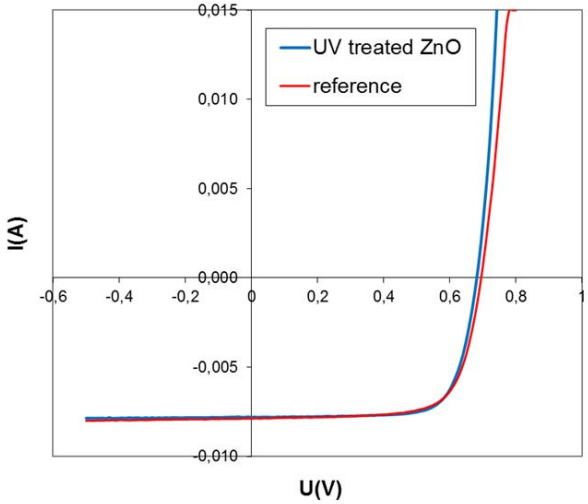


*Fig. 26: Measured (by ZSW) I-V curves for CIGS cell with UV treated un-doped ZnO TCO layer and reference CIGS cell with ZnO:Al TCO layer.*

# 4 Potential impact, main dissemination activities and exploitation of results

## 4.1 Potential impact

The hipoCIGS project has resulted in new material modifications and processes suitable for the industrial production of flexible, high-efficiency CIGS solar modules with a potential for reduction in production cost in future. The technical and economic assessment of the outcome, which was carried out by industrial project partners at the end of the project, has shown that the project developments offer process sequence for industrial roll-to-roll production of flexible CIGS modules as well as several development paths for reduction of production costs and improvement of conversion efficiency. The technologies developed in this project thus carry the potential for accelerated market penetration of cost-effective flexible solar modules. Besides opening up new markets where flexible and/or light-weight modules are a prerequisite, the intrinsic cost advantages of large-scale roll-to-roll production and the reduced balance-of-system costs associated with light-weight, large-area modules may in time also allow this technology to penetrate the huge market for large-scale PV power production that is currently covered by standard glass-based modules.

The impact of the sub-topics of this project will now be described in more detail:

- Different types of **flexible substrates** were investigated in this project. Of these, polyimide is ready for industrial roll-to-roll production with the current state of the art. Other substrates like mild steel and enamelled mild steel make it easier to achieve high efficiencies and thus offer a possible development path towards an even more cost-effective production.
- Flexible substrates usually require an external **Na supply** for good CIGS efficiencies, unlike glass substrates where Na can diffuse from the substrate. Several Na supply methods were shown to achieve the necessary doping at low production costs: Na-containing back contacts, Na co-evaporation during CIGS evaporation, and Na post-deposition treatment.
- **CIGS deposition** can take place at lower or higher substrate temperature, depending on the maximum temperature that the substrate can withstand. While high efficiencies can generally be realised more easily with a high-temperature process, the considerable improvements in the low-temperature process achieved within the project, including an 18.7% efficiency world record for cells on polyimide, demonstrate the potential of this process and thus open up a path for further cost reduction based on polyimide as an established substrate.
- Evaporated **$In_2S_3$ buffers** have been brought close to industrial applicability by this project. Although the CdS buffer currently used as a standard for CIGS devices is very thin and therefore contains only minute amounts of cadmium, a completely cadmium-free alternative is environmentally desirable and additionally gives access to markets in countries with strong legislative restrictions on the use of cadmium. Additionally, the CdS buffer is usually applied by chemical bath deposition (CBD), which is a wet chemical process and therefore of only limited compatibility with a continuous roll-to-roll production. $In_2S_3$ evaporation, on the other hand, can be integrated easily into a roll-to-roll production line, so beside the advantages of being cadmium-free, it will also reduce production costs further.

- **Interconnection** of many single cells is required in module production to achieve practicable values of voltage and current. For flexible CIGS, the standard approach used in several start-up companies still is to cut the substrate into single cells and connect these e.g. by busbars. A monolithically integrated interconnection, like it is used for thin-film solar technologies on glass substrates, is technologically more demanding, particularly on flexible substrates, but in the end offers a more cost-effective production method involving significantly less handling: The substrates can be processed completely by roll-to-roll technologies, and the roll can then be cut into modules close to the end of the process chain. A fully laser-based monolithic interconnect method was successfully established in this project for CIGS modules on polyimide substrate.

In addition to these results regarding industrial applicability, considerable progress was also achieved in other research areas as well. For example, excellent cell efficiencies were realised on different substrates using low-temperature CIGS deposition, and it was shown that efficiencies even higher than on glass substrate can be achieved using enamelled steel as a substrate, where the enamel composition can be tailored to act as a sodium source as well. The advancement in scientific understanding of – amongst other things – the role of sodium doping in CIGS and metastable cell behaviour will help to improve CIGS technology even further. These results and the accompanying knowledge gained during the project will aid European PV research to maintain a lead in CIGS technology.

## 4.2 Main dissemination activities

The project and its results were presented at numerous workshops and conferences worldwide, e.g. the European Photovoltaic Solar Energy Conference (EU-PVSEC) series, the International Photovoltaic Science and Engineering (PVSEC) conferences, the IEEE PV Specialists Conference, and several others. An invited presentation titled “New concepts for high efficiency and low cost inline manufactured flexible solar cells” was given at the PVSEC-22 in Hangzhou, China.

About 20 articles dealing with the project results were published in peer-reviewed scientific journals such as Progress in Photovoltaics, Nature Materials, IEEE Journal of Photovoltaics, and Thin Solid Films.

## 4.3 Exploitation of results

With Flisom, the project consortium includes an industrial partner who has already started industrialization efforts and is establishing prototype roll-to-roll production of flexible CIGS modules on polyimide. It is therefore natural that most of the project results can be exploited by Flisom. However most concepts still need adaption to roll-to-roll manufacturing. Possible exploitation of other results, especially on non-polyimide substrates, is currently being discussed among project partners; some of the topics will also be pursued further in the follow-up project R2R-CIGS. Additionally, Manz as a high-tech equipment manufacturer is capable and willing to exploit the project results by constructing appropriate production equipment for flexible CIGS modules. Tata Steel and Pemco on their side have strong interest in further development of substrates for CIGS PV applications.

hipoCIGS has helped project partners to refine technologies and explore alternative solutions. The project has enabled industrial partners to greatly improve manufacturing know-how. Industrial partners Flisom, Manz, Tata Steel, and Pemco have also been able to strengthen their collaboration in the area of high performance flexible CIGS modules.

Results obtained by the hipoCIGS project have strengthened the confidence of Flisom's investors that CIGS thin-film technology has great potential for low-cost renewable energy. Flisom is now engaged in an effort to convert its prototype roll-to-roll production line into a pilot line that will act as a blueprint for a future scaled-up manufacturing facility.

Thanks to hipoCIGS, the partners have:

- Evaluated polyimide substrates and established criteria for selection of polyimide films in production line,
- Improved their understanding of back-contact deposition parameters that influence handling performance,
- Increased know-how in the influence of CIGS thickness on photovoltaic efficiency and high growth rate deposition that will be highly valuable when tuning next production lines,
- Gained experience with an alternative buffer layer technology in case of required changes in composition to adopt $In_2S_3$ buffer,
- Obtained many results in the area of laser scribing that are being exploited in the follow-up FP7 R2R-CIGS project for the development of high throughput laser scribing systems,
- Compared various front-contact grid deposition techniques to be able to compose a range of flexible solar modules,
- Gained insight into various front-contact deposition technologies while tuning sputtering technique which will be used for future volume production.

In short, many hipoCIGS results are interesting for applicability in production line, either as equipment manufacturer like Manz or as solar modules manufacturer like Flisom. Results on substrates are also important for future plans and strategy of Tata Steel and Pemco. Some hipoCIGS results offer alternative know-how that may serve as back-up solutions or present potential for future R&D.

## Contact details

**Project website address: http://hipoCIGS.zsw-bw.de**

**Project partners and contact persons:**

| **Beneficiary name** | | |
|---|---|---|
| ZENTRUM FUER SONNENENERGIE- UND WASSERSTOFF-FORSCHUNG BADEN-WUERTTEMBERG (ZSW) | Industriestrasse 6<br>D-70565 Stuttgart<br>Germany | Friedrich Kessler<br>friedrich.kessler@zsw-bw.de |
| FLISOM AG (Flisom) | Ueberlandstrasse 129<br>CH-8600 Duebendorf<br>Switzerland | David Brémaud<br>david.bremaud@flisom.ch |
| TATA STEEL NEDERLAND TECHNOLOGY BV (TATA) | Tata Steel RD &T<br>IJmuiden Technology Center<br>PO Box 10000<br>1970 CA Ijmuiden<br>The Netherlands | Ganesan Palaniswamy<br>ganesan.palaniswamy@tatasteel.com |
| PEMCO BRUGGE BVBA (PEMCO) | Pemco Brugge BVBA<br>Pathoekeweg 116<br>B-8000 BRUGGE<br>Belgium | Christian Schlegel<br>Christian.Schlegel@pemco-intl.com |
| MANZ CIGS TECHNOLOGY GMBH (MCT) | Alfred-Leikam-Str. 25<br>D-74523 Schwaebisch Hall<br>Germany | Bernhard Dimmler<br>bdimmler@manz.com |
| EIDGENOESSISCHE MATERIALPRUEFUNGS- UND FORSCHUNGSANSTALT (EMPA) | EMPA<br>Laboratory for Thin Films and Photovoltaics (Abt. 130)<br>Ueberlandstr. 129<br>CH-8600 Duebendorf<br>Switzerland | Ayodhya Nath Tiwari<br>Ayodhya.Tiwari@empa.ch |
| NEDERLANDSE ORGANISATIE VOOR TOEGEPAST NATUURWETENSCHAPPELIJK ONDERZOEK (TNO) | TNO<br>Thin Film Technology<br>P.O. Box 6235<br>NL-5600 HE Eindhoven<br>The Netherlands | Pieter Jan Bolt<br>pieter_jan.bolt@tno.nl |
| POLITECHNIKA WARSZAWSKA (WUT – Warsaw University of Technology) | Warsaw University of Technology<br>Faculty of Physics<br>Koszykowa 75<br>00-662 Warszawa<br>Poland | Malgorzata Igalson<br>igalson@if.pw.edu.pl |